Control of angular momentum evolution in Stark wave packets

H. Wen, C. Rangan, and P. H. Bucksbaum
FOCUS Center, Department of Physics, University of Michigan, Ann Arbor, Michigan 48109-1120, USA
(Received 24 June 2003; published 14 November 2003)

Using techniques of ultrafast coherent control, we propose a method to produce high-purity high-ℓ (angular momentum) states in Rydberg Stark wave packets. Two time-delayed phase-locked laser pulses excite the atom from a low-lying ''launch state'' into a low-ℓ Rydberg wave packet, in the presence of a static electric field. By choosing the time delays between the pulses, and the static electric field, we find that a high-ℓ state with high purity can be created at the target time.

DOI: 10.1103/PhysRevA.68.053405 PACS number(s): 32.80.Qk, 32.80.Rm, 32.60.+i

I. INTRODUCTION

Rydberg atoms are important model systems to explore and elucidate aspects of quantum dynamics. Ultrafast laser excitation of a Rydberg atom generates an electronic wave packet composed of a coherent superposition of several eigenstates. Studies of wave packet dynamics [1–4] have revealed both their particlelike behavior such as localization [5], and their wavelike behavior such as fractional revivals [6]. The dynamics of wave packets can be enriched by external fields that break the spherical symmetry of the Coulomb potential. For example, Stark wave packets exhibit angular momentum revivals [7,8], which have been explained by simple classical models [10]. Nonhydrogenic features of alkali-metal Stark spectra have been understood in terms of semiclassical models of core scattering [9]. In this paper, we extend the study of angular momentum evolution in Stark wave packets and suggest a simple scheme for its control.

Wave packet control of the principal quantum number n has been used for the storage and retrieval of information in Rydberg atom data registers [11–13]. In Stark wave packets, the parabolic quantum number k could be used as a second degree of freedom for quantum information processing. The control of both the radial and angular evolution would allow us to produce atomic wave packets correlated in two degrees of freedom n and k, to facilitate more complex quantum information processes [14].

In this paper we propose to use the angular momentum represented by the quantum number ℓ as the second degree of freedom for a Stark wave packet. Even though angular momentum does not commute with the Stark Hamiltonian, and therefore is not stationary, we nonetheless find that we can produce high-purity ℓ states at a target time using a series of ultrafast pulses.

This paper is organized as follows. In Sec. II, we study the dynamics of an electronic wave packet in an external static electric field. In Sec. III, a pair of phase-locked laser pulses is employed to excite two electronic wave packets with relative phase δ and delay time τ. Specific angular momentum states can be obtained by choosing the pulse parameters δ and τ appropriately. Further discussion and conclusions are presented in Sec. IV.

II. DYNAMICS OF ANGULAR MOMENTUM COMPONENTS IN STARK WAVE PACKETS

A one-electron atom in a static electric field F is described by the time-independent Hamiltonian $H=p^2/2+V(r)+Fz$ (in atomic units). The static electric field breaks the spherical symmetry of the Coulomb potential, and the angular momentum ℓ is no longer a good quantum number. The eigenstates of the Stark Hamiltonian are denoted by $|nk\rangle$, where k is a label for the Stark eigenstates in parabolic coordinates [15].

A Stark wave packet is a coherent superposition of Stark eigenstates written as

$$|\Psi\rangle=\sum_{nk} a_{nk}|nk\rangle. \tag{1}$$

Its time evolution is written as

$$|\Psi(t)\rangle=\sum_{nk} a_{nk}e^{-iw_{nk}t}|nk\rangle. \tag{2}$$

Each of the Stark eigenstates $|nk\rangle$ can be expanded in the $|n\ell m\rangle$ basis of the field-free Hamiltonian as $|nk\rangle=\Sigma_{n\ell}c_{n\ell}^{nk}|n\ell\rangle$ and each carries different angular momentum components (the magnetic quantum number m is conserved and chosen to be $m=0$). In the wave packet, quantum interference between these eigenstates leads to the precession of angular momentum.

We start the discussion with the simplest atom, hydrogen. Spin-orbit coupling is neglected throughout this paper, because the small spin-orbit splitting contributes negligible dephasing over the evolution time of interest for these wave packets. The energy of hydrogen in an electric field F is given to first order by

$$W=-\frac{1}{2n^2}+\frac{3nFk}{2} \tag{3}$$

$$=\omega_0+k\Delta E, \tag{4}$$

where k is the state index that runs between $-(n-1)$, $-(n-3),\ldots,(n-3),(n-1)$. Since no quantum defects are involved, the first-order energy levels w_{nk} are separated symmetrically around $W=-1/2n^2$. The eigenvectors $|nk\rangle$ expanded in the $|n\ell\rangle$ basis can be computed analytically [15]. Assuming only one n manifold is excited, the expectation value of the L^2 operator evolves in time as

$$\langle\Psi(t)|L^2|\Psi(t)\rangle=\sum_{k',k} a_{nk'}^{*}a_{nk}e^{i(w_{nk'}-w_{nk})t} \times\sum_{\ell} c_{n\ell}^{*nk'}c_{n\ell}^{nk}\ell(\ell+1). \tag{5}$$

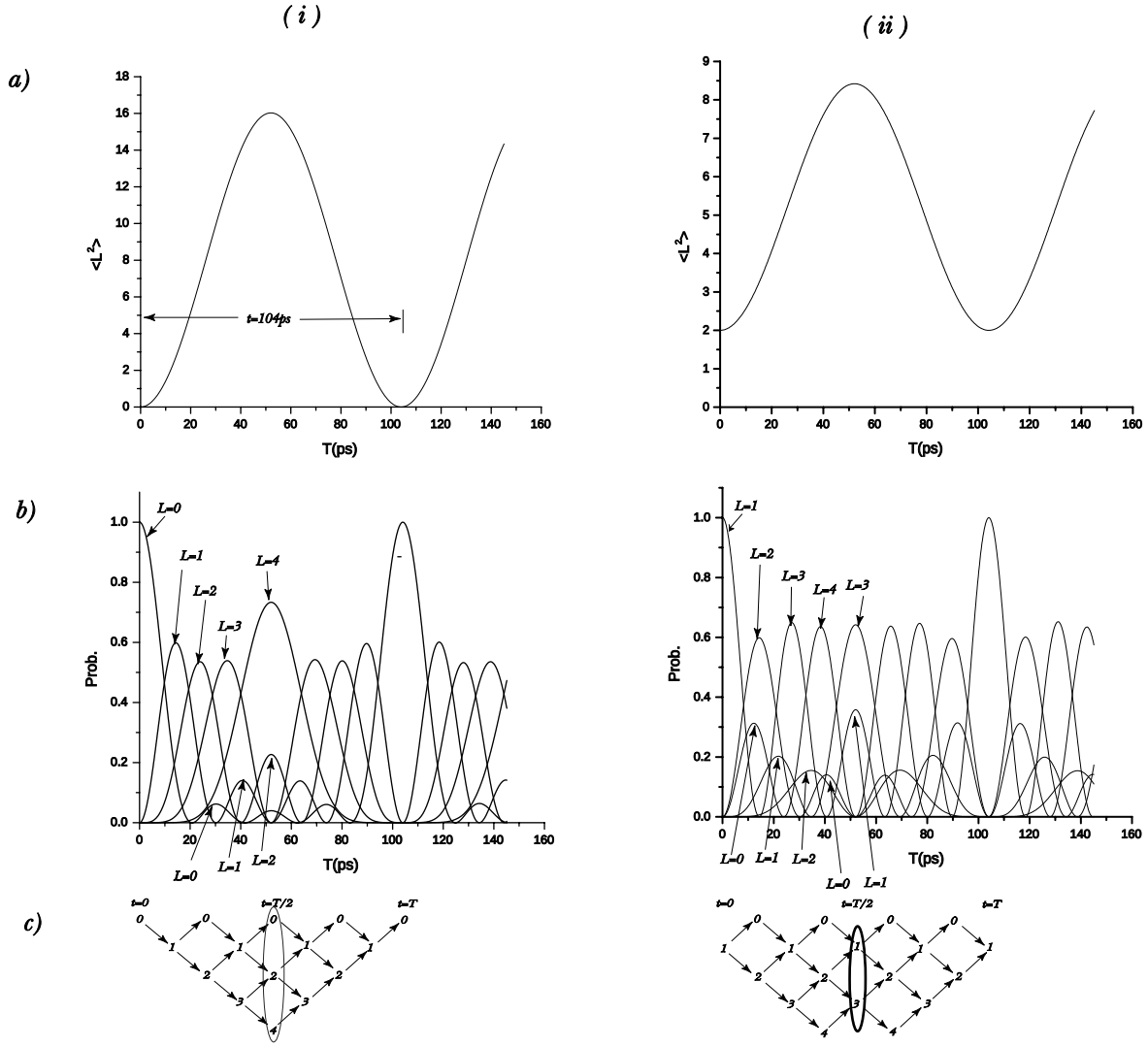

FIG. 1. The dynamics of angular momentum evolution in the $n=5$ manifold of hydrogen atoms in an external dc electric field $F=500$ V/cm. (a) The evolution of observable $\langle L^2\rangle$; (b) the evolution of angular momentum composition for individual ℓ states; (c) the diagram to illustrate the quantum properties of the evolution. Arrows indicate the dipole coupling due to the electric field. The ellipses indicate the ℓ components that get population at half of the evolution period. Column (i) is the plots where the initial state carries only pure $\ell=0$ component; column (ii) is the plots where the initial state carries only pure $\ell=1$ component.

For simplicity of discussion, we choose an $n=5$ wave packet in this section, but the arguments are generally valid for arbitrary n as seen in the next section. The calculated evolution of $\langle L^2(t)\rangle$ is plotted in Fig. 1(a)(i) and Fig. 1(a)(ii), taking pure s and p states as the initial states, respectively. Their periodic structures reveal the classical properties of the wave packets. In a simple classical model, an electron bound to the nucleus experiences a torque $\vec{\tau}=-\vec{r}\times\vec{F}$ due to the external electric field. In the first half of the revival period, $\vec{\tau}\cdot\vec{L}>0$, and the torque increases the magnitude of $\vec{L}$, while in the second half of the revival period, $\vec{\tau}\cdot\vec{L}<0$, and the torque decreases the magnitude of $\vec{L}$. Therefore, the electric field drives the magnitude of $\vec{L}$ to its maximum value at time $t_{ang}/2$ and brings it down to the low angular momentum at t_{ang}, provided the initial state carries low-angular-momentum components. This has been observed in experiments on atomic Rydberg states in atomic beams [7,8]. The frequency of the $\langle L^2(t)\rangle$ oscillation is governed by the energy difference between the nearest-neighbor Stark states $\Delta E=W_{n,k}-W_{n,k-1}=3Fn$, leading to the angular momentum revival time $\tau_{ang}=2\pi/3nF$.

This periodicity can be seen explicitly in the time evolution of the wave packet as shown below. For compactness of notation, we drop the subscript n when we refer to a wave packet with states from the same n manifold.

$$|\Psi(t\pm\tau_{ang})\rangle=\sum_k a_k e^{-i\omega_k(t\pm\tau_{ang})}|k\rangle \tag{6}$$

$$=\sum_k a_k e^{-i\omega_k t}e^{\mp i\omega_k\tau_{ang}}|k\rangle \tag{7}$$

$$= \sum_k a_k e^{-i\omega_k t} e^{\mp i(\omega_0 + k\Delta E)\tau_{ang}} |k\rangle \tag{8}$$

$$= \sum_k a_k e^{-i\omega_k t} e^{\mp i\omega_0 \tau_{ang}} e^{\mp ik\Delta E \tau_{ang}} |k\rangle \tag{9}$$

$$= e^{\mp i\omega_0 \tau_{ang}} \sum_k a_k e^{-i\omega_k t} e^{\mp i2\pi k} |k\rangle \tag{10}$$

$$= e^{\mp i\omega_0 \tau_{ang}} |\Psi(t)\rangle. \tag{11}$$

So the classical revival of the wave function is good only up to an overall phase, and, as shown in Ref. [16], it is dependent on the energy level separations being roughly equal.

Now, we examine the evolution of angular momentum in the Stark Rydberg wave packet. The evolution of a particular ℓ component in the wave packet is given by

$$P_\ell = |\langle n\ell|\Psi(t)\rangle|^2 = \left| \sum_k a_{nk} e^{-iw_{nk}t} c_{nl}^{nk} \right|^2. \tag{12}$$

Figure 1(b)(i) shows all ℓ components of the wave packet with the initial $P_{\ell=0}(t=0)=1$ as a function of time. As the classical value of $\langle L^2(t)\rangle$ increases from its initial low value, the wave packet ℓ component distribution changes as well: i.e., the dominant ℓ component goes from low ℓ to high ℓ in a sequence that we call the strongest revival sequence. (Here we define the revival sequence as a set of revival peaks of different ℓ components in sequence.) The angular momentum revival time is $\tau_{ang}=2\pi/3nF=104$ ps for $n=5$ and $F=500$ V/cm as already seen in the $\langle L^2(t)\rangle$ plot.

The evolution of angular momentum components shows other interesting properties. A weaker revival sequence starting after the first sequence is also evident. The presence of two different sequences can be traced to the dipole coupling properties of angular momentum states. The external electric field couples each ℓ to its neighbors ($\ell \pm 1$) according to the dipole selection rule, except for $\ell=0$ and $\ell=n-1$, which form ℓ ''boundaries.'' These coupling ''paths'' are shown schematically in Fig. 1(c). The strong revival sequence in Fig. 1(b) goes along the path on the bottom-most edge of the graph in Fig. 1(c). The weaker one goes along the path parallel with the previous path in Fig. 1(c). It is interesting to note that there are int$[n/2]$ such paths and hence int$[n/2]$ revival sequences for a Stark wave packet in a particular n manifold.

The value of ℓ at the classical maximum, halfway through the angular momentum precession period, depends on several factors. In general, through one full angular momentum period there are $2(n-1)$ changes in ℓ. Therefore, in half this period, there are $n-1$ changes in ℓ. Consequently, if the initial ℓ is even (odd) and n is odd (even), the only populated ℓ at $t=\tau_{ang}/2$ will be even ℓ's; if the initial ℓ is even (odd) and n is even (odd), the only populated ℓ at $t=\tau_{ang}/2$ will be odd ℓ's. Classically, we always expect that the highest ℓ state ($\ell=n-1$) should dominate at $t=\tau_{ang}/2$ to maximize $\langle L^2(t)\rangle$. This behavior is observed in a wave packet starting from a pure s state as seen in Fig. 1(b)(i). However, this behavior is not always observed as shown in Fig. 1(b)(ii)—when the initial ℓ is odd, at half the revival time, the $\ell=n-1$ component has zero population, even though the average angular momentum is a maximum.

Alkali-metal atoms behave similarly to hydrogen, except for low-ℓ components for which quantum defects are not negligible. These low-ℓ states are separated from the rest of the Stark manifold. During angular momentum evolution, the low-ℓ components are relatively ''conserved.'' As an example, we calculated the wave packet evolution in a lithium atom generated by exciting the atom from the $3p$ state to the $n=25$ manifold using a Gaussian pulse. Since the pulse duration is much smaller than τ_{ang}, the angular momentum components of the wave packet are frozen during the excitation; so the initial wave packet contains only s and d components. As Fig. 2(a) shows, the probability of the low-ℓ components, which do not mix with the other ℓ states, never goes to zero. The evolution of the $\ell=10$ component is illustrated separately in Fig. 2(b) and is representative of the intermediate ℓ components. The evolution of high-ℓ states is shown in Fig. 2(c), and this shows the wavelike behavior described in the previous paragraphs.

In a wave mechanical view, each Stark eigenstate $|nk\rangle$ carries all ℓ components. The coherent evolution of the wave packet leads to the constructive interference between some ℓ components and the destructive interference of others, which leads to the evolution of angular momentum in Stark wave packets. By a coherent superposition of the Stark eigenstates, it is possible to produce a high-purity high-ℓ state, which leads the discussion in Sec. III.

III. PRODUCING ARBITRARY HIGH-ℓ STATES

General laser excitation schemes which excite from low-lying low-ℓ states with only a few photons are limited to low-angular-momentum states by angular momentum selection rules. Making high-ℓ Rydberg states is challenging. The key is to break the spherical symmetry of the Coulomb potential, thus causing the evolution of angular momentum. Most schemes to make high-ℓ states are based on this principle. For instance, the adiabatic rf dressing method [17] uses a rf field to break the symmetry and adiabatic passage to evolve the angular momentum to the desired value. The crossed fields method [18] employs both electric and magnetic fields to break the symmetry. In the strong-laser excitation scheme, the fast oscillating laser field breaks the symmetry by causing ac Stark shifts and consequent angular momentum evolution [19–21]. A recent report demonstrates control of low-angular-momentum composition, rooted in symmetry breaking by quantum defects [22]. These schemes are not generally able to achieve a full control of angular momentum composition, although some of them can produce particular states such as circular states with high probability. Here, we present a general scheme to make *arbitrary* angular momentum states within a certain range, even those with nearly pure high ℓ in particular circumstances, by a pair of phase-locked laser pulses.

In Sec. II, we saw that each ℓ component is significant once or twice in a full revival period (see Fig. 2) with rela-

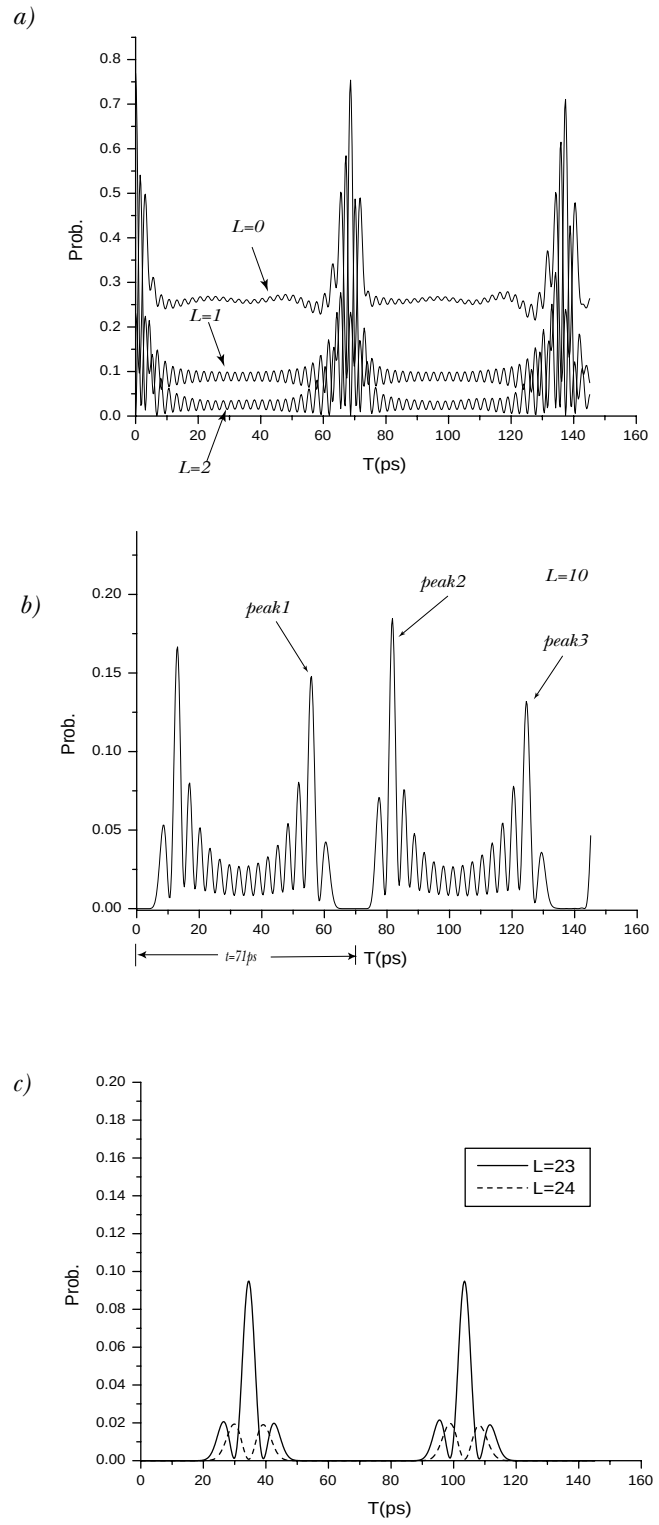

FIG. 2. The dynamics of angular momentum evolution in the $n=25$ manifold of lithium atoms in a dc electric field $F=150$ V/cm. The initial state is the superposition of $25s$ and $25d$ states after the excitation from the $3p$ launch state. (a) The population of low-ℓ states where quantum defects are not negligible; (b) the population of $\ell=10$ states; (c) the population of high-ℓ states.

tively low population. This can be understood using the following analysis. A particular ℓ component dominates at times $\tau_{ang}+t$ and $\tau_{ang}-t$. The time-dependent wave function at these times can be written as

$$|\Psi(\tau_{ang}\pm t)\rangle = e^{i\omega_0\tau_{ang}}|\Psi(\pm t)\rangle. \tag{13}$$

Also,

$$A_\ell(\tau_{ang}\pm t)=\langle \ell|\Psi(\tau_{ang}\pm t)\rangle = e^{i\omega_0\tau_{ang}}\sum_k c_k^{*\ell}a_k e^{\mp i\omega_k t} \tag{14}$$

$$= e^{i\omega_0\tau_{ang}}\sum_k c_k^{*\ell}a_k e^{\mp i(\omega_0+k\Delta E)t} \tag{15}$$

$$= e^{i\omega_0(\tau_{ang}\mp t)}\sum_k c_k^{*\ell}a_k e^{\mp ik\Delta E t}. \tag{16}$$

For Stark states, the energies are symmetrically split around ω_0. So for every k term there is an opposite $-k$ term and C_{-k} equals a_k since all the excitations we have considered are Gaussian. Also, the ℓ components of the downhill states are equal to the ℓ components of the uphill states, i.e., $c_{-k}^{*\ell}=c_k^{*\ell}$. This explains why we see a symmetric revival of ℓ states within each angular momentum period. This also suggests that the control scheme may not work in some cases in which $C_{-k}a_{-k}^{*\ell}$ is not equal to $C_k a_k^{*\ell}$.

High population for the target ℓ may be obtained by enhancing the probability of the target ℓ at the expense of other ℓ components. We can do this via wave packet interference. If the overall phase between two identical, time-delayed wave packets is chosen properly, constructive interference occurs for the target ℓ and destructive interference for other ℓ states, leading to significant enhancement of the target ℓ population. For maximum effect, the second laser pulse must excite the second wave packet at a specially selected delay time τ such that the target ℓ dominates in both wave packets at time t. We start with the initial state as

$$|\Psi(t)\rangle = \sum_\ell \beta_\ell(t)|n\ell\rangle, \tag{17}$$

where $\beta_\ell(t)=\Sigma_k c_{nk}e^{-iw_{nk}t}a_{n\ell}^{*k}$. After a delay time τ, a second wave packet is excited with an overall phase difference δ from the first. Therefore, the final wave packet at a target time t can be written as

$$|\Psi(t,\tau,\delta)\rangle = \sum_\ell \beta_\ell(t)|n\ell\rangle + e^{i\delta}\sum_\ell \beta_\ell(t+\tau)|n\ell\rangle. \tag{18}$$

We assume that only a small amount of population is excited to the Rydberg series and the ground state always has almost unity population. Thus, up to a normalization factor $N(\tau,\delta)$ for Rydberg series, the probability of the ℓ component is

$$P_\ell(t,\tau,\delta)=\frac{|\beta_\ell(t)+e^{i\delta}\beta_\ell(t-\tau)|^2}{N^2}. \tag{19}$$

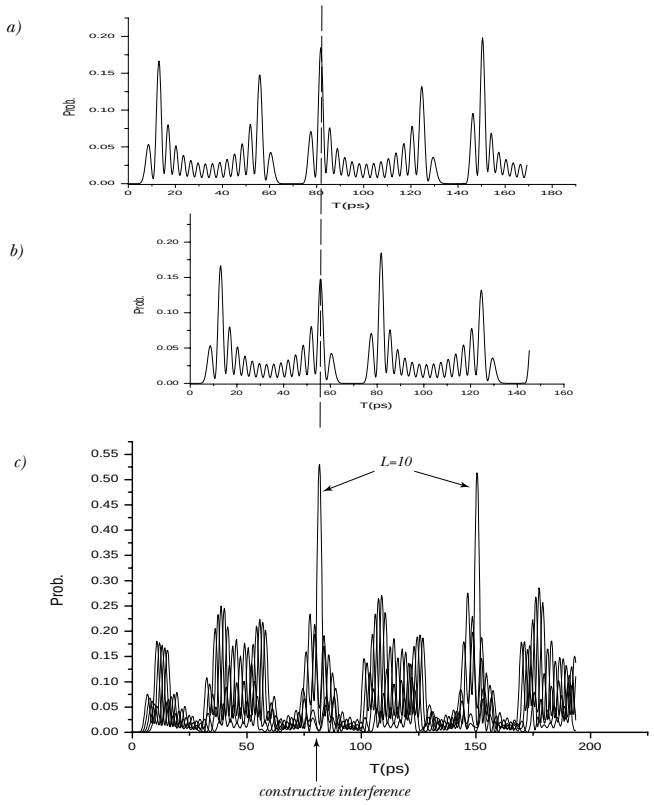

FIG. 3. The scheme to produce high population for $\ell=10$ state in lithium Rydberg wave packets. (a) The single wave packet evolution; (b) the second wave packet evolution, which is generated at time delay τ with relative phase δ; (c) the population of $\ell=10$ stands out compared with its neighbors ($\ell=8,9,11,12$) at the designed observation time $t=81$ ps.

We can illustrate this method with the previous example of an $n=25$ lithium wave packet consisting of only s and d components initially. The target is a pure $\ell=10$ state. Figure 2(b) shows that there are two peaks of the $\ell=10$ population within one angular revival period. We label the peak at time $t-\tau_{ang}$ as peak$_1$ and the peak at time $t+\tau_{ang}$ as peak$_2$.

After generating the first wave packet, peak$_2$ appears at $t=81.76$ ps. The second wave packet is excited after a delay of $\tau=51.12$ ps so that its peak$_1$ can be expected at the same time of $t=81.76$ ps. The two wave packets interfere with each other to enhance or suppress the $\ell=10$ components at this target time, depending on their relative phase.

In the pulse-interference plot [Fig. 3(c)], the $\ell=10$ component stands out from its neighbors with normalized probability 0.52 at target time. We can perform a search to identify the value of δ that leads to maximum constructive interference for $\ell=10$. In a three-dimensional (3D) plot of t, δ, and P_{10} (Fig. 4), the probability of $\ell=10$ varies as a function of δ. By changing the relative phase δ, we can achieve a good amount of control over generating high-angular-momentum states.

In the discussion above, the delay time τ is fixed at the value suggested by the revival pattern for the designated ℓ. Is it possible to achieve better enhancement of the target ℓ with a different delay time τ? To help answer this question,

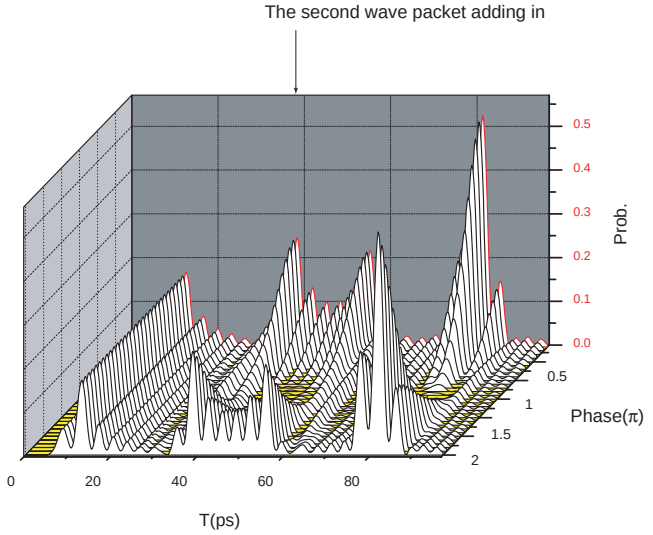

FIG. 4. A 3D plot of t, δ, and probability of $\ell=10$, in which the delay time τ is fixed.

we performed a search for the optimal values of τ, δ, and t. The conclusion is that for two pulses the optimal time delay is indeed the one suggested by the revivals. The presence of at least two revival peaks for the target ℓ is critical. No enhancement is possible for two pulses separated by τ_{ang}, since then the two wave packets are identical up to an overall phase. Therefore the normalized population of the target ℓ can only be the same as that in the single pulse case.

In this simple two-pulse scheme to produce high-ℓ states, the maximum probability for target states depends on the strength of the two revivals. Most of the high-ℓ components in the lithium wave packets for $n=25$ can be enhanced to around 0.5 probability; but the maximum population of the $\ell=24$ ''circular'' state (i.e., $\ell=n-1$) is only 0.17, since the peak amplitudes in one wave packet are quite low. However, this failure to produce a high-purity $\ell=n-1$ state is not a general feature of this scheme. For instance, consider an initial $n=7$ state in hydrogen containing only a pure s component excited at $t=0$. The maximum probability for $\ell=6$ during the angular momentum precession is 0.63. When a second wave packet is launched at delay $\tau=15$ ps, $F=500$ V/cm, with relative phase $\delta=1.6755$ rad, we find that at observation time $t=96$ ps, the wave packet $\ell=6$ component peaks with probability 0.97.

This process of producing arbitrary angular momentum states can be written in the formalism of wave packet interference control. Our aim here is to start from a superposition of Stark states that gives us the initial angular momentum state and produce a specific superposition of Stark states that gives us a different angular momentum state. That is, the initial state $\Psi_i=\Sigma_k C_k|k\rangle$ must be transformed to a different state $\Psi_f=\Sigma_k D_k|k\rangle$. The initial wave packet Ψ_i is normalized to 1, i.e., $\Sigma_k|C_k|^2=1$. When two such wave packets with a time delay τ and a relative phase δ interfere with each other, the wave packet at a target time T is written as

$$|\Psi_f(T)\rangle=|\Psi_i(T)\rangle+e^{i\delta}|\Psi_i(T-\tau)\rangle \tag{20}$$

$$= \sum_k \ (1 + e^{i(\delta + w_{nk}\tau)}) C_{nk} e^{-iw_{nk}T} |nk\rangle. \quad (21)$$

The normalization constant N is a function of both τ and δ:

$$N^2 = \langle \Psi_f(T) | \Psi_f(T) \rangle = 2 \sum_k \ [1 + \cos(\delta + w_{nk}\tau)] |C_k|^2. \quad (22)$$

The normalized wave function at time T is written as

$$|\Psi_f(T)\rangle = \frac{1}{N} \sum_k \ (1 + e^{i(\delta + w_{nk}\tau)}) C_{nk} e^{-iw_{nk}T} |nk\rangle. \quad (23)$$

The term $e^{-iw_{nk}T}$ is simply the phase evolution. The population in the kth eigenstate is given by

$$|C_k(T)|^2 = \frac{1}{N^2} \ 2[1 + \cos(\delta + w_{nk}\tau)]. \quad (24)$$

One necessary condition to produce the appropriate ℓ is to make $|C_k|^2$ equal to $|D_k|^2$ for every k. This is a k-dimensional optimization problem, which does not have a simple solution. However, we may set some limits on the controllability of ℓ states. When $\tau = m\tau_{ang}$ and $\delta = 2\pi n$, then, as we said before, $C_k(T) = C_k$, and we get no enhancement. $|C_k(T)|^2$ can take a range of values between 0 and $(4/N^2)|C_k|^2$. If the populations of the components $|D_k|^2$ of the target angular momentum state lie within this range, there is a possibility that the desired angular momentum state can be produced.

In the experiments described in Ref. [22], arbitrary low-ℓ (s and d) wave packets in alkali metals can be created since they can be resolved spectroscopically, and their individual phases can be manipulated. However, that scheme cannot be used to produce arbitrary higher-ℓ states, which do not have a quantum defect. In our scheme, we are able to produce any ℓ state, albeit not with 100% probability. This is a contrast between coherent control in the frequency domain versus wave packet interference control.

IV. CONCLUSIONS

In conclusion, we have studied the dynamics of angular momentum in Stark wave packets in alkali-metal atoms. We propose an experimental scheme to control the angular momentum composition. Phase-locked laser pulses are employed to excite two Rydberg wave packets separated by a delay time τ, which interfere with each other constructively to produce a target ℓ state at a desired time by choosing the proper phase difference δ. Using this technique, even high-ℓ states can be created. It is well known that the measurement of high-ℓ Rydberg states is challenging. We are investigating several schemes to perform this measurement.

ACKNOWLEDGMENTS

It is a pleasure to thank Joel Murray for useful discussions and help. C.R. gratefully acknowledges support from the NSF FOCUS Center. This work was supported by the National Science Foundation under Grant No. 9987916 and the Army Research Office Grant No. DAAD 19-00-1-0370.

[1] J. Parker and C.R. Stroud, Jr., Phys. Rev. Lett. **56**, 716 (1986).
[2] J.A. Yeazell, M. Mallalieu, J. Parker, and C.R. Stroud, Jr., Phys. Rev. A **40**, 5040 (1989).
[3] C. Raman, C.W.S. Conover, C.I. Sukenik, and P.H. Bucksbaum, Phys. Rev. Lett. **76**, 2436 (1996).
[4] C. Raman, T.C. Weinacht, and P.H. Bucksbaum, Phys. Rev. A **55**, 3995 (1997).
[5] J.A. Yeazell and C.R. Stroud, Jr., Phys. Rev. Lett. **60**, 1494 (1988).
[6] J.A. Yeazell and C.R. Stroud, Jr., Phys. Rev. A **43**, 5153 (1991).
[7] A. tenWolde *et al.*, Phys. Rev. Lett. **61**, 2099 (1988).
[8] M.L. Naudeau, C.I. Sukenik, and P.H. Bucksbaum, Phys. Rev. A **56**, 636 (1997).
[9] M. Courtney, N. Spellmeyer, H. Jiao, and D. Kleppner, Phys. Rev. A **51**, 3604 (1995).
[10] P. Bellomo, C.R. Stroud, Jr., D. Farrelly, and T. Uzer, Phys. Rev. A **58**, 3896 (1989).
[11] J. Ahn, T.C. Weinacht, and P.H. Bucksbaum, Science **287**, 463 (2000).
[12] J. Ahn, D.N. Hutchinson, C. Rangan, and P.H. Bucksbaum, Phys. Rev. Lett. **86**, 1179 (2001).
[13] C. Rangan, J. Ahn, D. Hutchinson, and P.H. Bucksbaum, J. Mod. Opt. **49**, 2239 (2003).
[14] P. W. Shor, in *Proceedings of the 35th Annual Symposium on the Foundations of Computer Science*, edited by S. Goldwasser (IEEE Computer Society, Los Alamitos, CA, 1994).
[15] T. F. Gallagher, *Rydberg Atoms* (Cambridge University Press, Cambridge, England, 1994).
[16] I.Sh. Averbukh and N.F. Perel'man, Sov. Phys. Usp. **34**, 572 (1991).
[17] W.A. Molander, C.R. Stroud, Jr., and J.A. Yeazell, J. Phys. B **19**, L461 (1986).
[18] J. Hare, M. Gross, P. Goy, and Phys. Rev. Lett. **61**, 1938 (1988).
[19] R. Grobe, G. Leuchs, and K. Rzazewski, Phys. Rev. A **34**, 1188 (1986).
[20] J.D. Corless and C.R. Stroud, Jr., Phys. Rev. Lett. **79**, 637 (1997).
[21] H.M. Nilsen, J.P. Hansen, S. Selsto, and L.B. Madsen, J. Phys. B **32**, 4995 (1999).
[22] J.R.R. Verlet, V.G. Stavros, R.S. Minns, and H.H. Fielding, Phys. Rev. Lett. **89**, 263004 (2002).